PNAS
www.pnas.org

Supplementary Information for

Alpine ice evidence of a three-fold increase in atmospheric iodine deposition since 1950 in Europe due to increasing oceanic emissions

Michel Legrand, Joseph R. McConnell, Susanne Preunkert, Monica Arienzo, Nathan Chellman, Kelly Gleason, Tomás Sherwen, Mat J. Evans, Lucy J. Carpenter

Michel Legrand
Email: michel.legrand@univ-grenoble-alpes.fr

This PDF file includes:

Supplementary text
Figs. S1 to S8
Tables S1
References for SI reference citations

www.pnas.org/cgi/doi/10.1073/pnas.1809867115

Supplementary Information Text

Comparison of ion chromatography (IC) and continuous flow analysis (CFA) data

As seen in Fig. S1, the agreement between IC and CFA measurements on the C10 core is good for ammonium, nitrate, and sulfate.

Surface snow accumulation rates, firn, and post-deposition remobilization

Among impurities present in snow and ice, some species are reversibly trapped in snow and can be remobilized after snow deposition, particularly at polar sites characterized by low snow precipitation amounts. Post-depositional effects are expected to occur for species initially present in the atmosphere in the gas phase. Such effects have been extensively studied for H_2O_2 and HCHO (Hutterli et al., 2003). Several inorganic (HNO_3 and HCl) and organic acids (HCOOH and CH_3COOH) also experience remobilization after snow deposition (Legrand et al., 1996). Still rare are studies of iodine in snow and ice from polar regions, but those that have been conducted found seasonal variations characterized by a maximum concentration in winter, suggesting that summer iodine is lost because of photochemical IO recycling in the snowpack. A winter iodine maximum was observed in a snowpit sampled at Neumayer (coastal Antarctica, snow accumulation of 0.45 mwe yr^{-1}) by Frieß et al. (2000) and at Law Dome (coastal Antarctica, 0.63 mwe yr^{-1}) by Spolaor et al. (2014).

Firn and ice cores extracted from various Greenland sites have been analysed at DRI, including iodine measurements (Maselli et al., 2017). Characterized by annual snow accumulation rates ranging from ~0.10 to 0.40 mwe yr^{-1}, sites include B19 (70° 0'N, 36° 24'W, 0.098 m we yr^{-1}), Summit (72° 36′ N, 38° 18′ W, 0.21 mwe yr^{-1}), and D4 (71° 24′ N, 43° 54′ W, 0.393 mwe yr^{-1}) and these cores permitted investigation of possible iodine post-depositional processes. Fig. S2 shows the iodine level in Greenland ice is 12 times lower at the B19 site characterized by a low snow accumulation rate (0.098 mwe yr^{-1}) than at the D4 site (snow accumulation rate of 0.393 mwe yr^{-1}), and eight times lower than at Summit (snow accumulation rate of 0.21 m we yr^{-1}). This dependence of the iodine content of ice to the annual snow deposition at the site suggests a loss of iodine from the snow-pack at low snow accumulation sites. Furthermore, Fig. S2 reveals regardless of site a systematic decrease in the iodine content of firn compared to that of ice with the decreases taking place suddenly in layers having a density close to 0.83 g cm^{-3}. This pattern suggests that a significant fraction of iodine has escaped from firn cores by volatilization either during storage or melting of firn during analysis. Note that with the DRI continuous ice core analytical, elemental analyses are conducted ~4 minutes after initial melting.

The net surface snow accumulation rates observed in the vicinity of the Col du Dome (CDD) drill site remain far larger than those encountered in polar regions (i.e. >0.50 mwe yr^{-1}) and may limit post-depositional remobilization of volatile species in a large upper part of the core. Previous studies conducted on the CDD ice cores explored the importance of post depositional remobilization of some volatile species. For nitrate, Preunkert et al. (2003) showed that the well-marked seasonal cycle characterized by a summer maximum is preserved back to 86 mwe depth. For acetic acid and to a lesser extent formic acid, however, Legrand et al. (2003) reported that these species do not

exhibit a clear seasonal cycle along the whole CDD ice core. Still present near the surface, the seasonal cycle of acetic acid tends to vanish further down the core, particularly in snow layers characterized by enhanced acidity from large NO_x and SO_2 emissions (i.e., the 1950s to 1980s). Finally, as discussed by Legrand et al. (2013), among all species that were investigated in the CDD ice, HCHO stands out with a total absence of seasonality in contrast to a summer maximum observed in the atmosphere at sites located at middle elevations in Europe. For instance, a summer-to-winter ratio of three was observed at the Zugspitze Alpine site located at 2650 m asl (Leuchner et al., 2016). Given high volatility of some of the iodine species present in the atmosphere (HOI), we will carefully examine in the following the possible effect on the observed iodine trends of the decrease with depth of net snow accumulation rates along the CDD cores related to changing origin of the ice.

It has here to be emphasized that the most abundant iodine species in the pre-industrial atmosphere, HOI, is a very weak acid (pKa = 10.5). Therefore, in contrast to other weak acids like formic and acetic acids, we do not expect a pH dependence incorporation of this gas into hydrometeor. Thus, the increased acidity of the atmosphere after 1950 resulting from growing NO_x and SO_2 anthropogenic emissions would have little impact on incorporation of iodine into precipitation. Also, as discussed in the SI Appendix, the presence of alkaline layers related to Saharan dust events occasionally reaching the CDD site did not significantly affect the iodine concentrations in ice.

We also restricted our CDD measurements to cores with density >0.70 g cm^{-3} (i.e., ice and dense firn) to minimize (avoid) any bias related to loss of iodine from firn during storage or analysis of cores as seen for Greenland cores. Individual half-year summer and winter iodine means are reported in Fig. S3, together with annual, winter, and summer ice-layer thicknesses from 1890 to 2000. In this figure, the iodine concentrations observed in layers having a density lower than 0.83 are reported as open symbols. For winter layers, it can be seen that, the iodine concentrations in firn (winters 1978/79, 1979/80, 1995/96, 1996/97, 1997/98, and 1998/99) are rather low compared to those in neighbouring ice layers. The difference between firn layers (1979, 1980, 1981, 1996, 1997, 1998, and 1999) is less obvious in summer. These lower losses from firn in summer than in winter may be due to the presence of ice lenses formed by refreezing of percolated water in summer. For safety, firn data were not considered in our analyses.

As discussed above, observations suggest that iodine concentrations in Greenland ice are dependent on the annual snowfall rate, with post-deposition remobilization and loss to the atmosphere the likely cause at least at sites with annual snowfall rates between 0.10 and 0.40 mwe yr^{-1}. While iodine concentrations in the CDD ice layers increased through time, this increase was parallel to an increase in annual ice layer thickness (ILT), from 0.5 mwe between 1930 and 1950 to 1.5 mwe between 1965 and 1980 (Fig S3). Ice flow thinning, which is particularly pronounced in small alpine glaciers such as this, means that annual ILT in the core is substantially less than the amount of snow deposited at the surface each year. For example, model simulations (Gilbert et al., 2014) indicate that the 1930 to 1950 annual layers in CDD have been thinned by ~50%. Because of the uncertainties associated with ice flow modelling of complex mountain glaciers, however, we primarily used ILT observed in the core in our interpretation rather than annual snowfall. To distinguish changes in atmospheric iodine levels through time from potential

effects of changing snow deposition rate, we evaluated the iodine record in the ice for different ranges of annual ILT.

During the earliest 40 years of the record (1890-1930), the mean annual ice thickness was only ~0.14 ± 0.08 mwe. After considering ice thinning, these values likely correspond to surface snow accumulation rates ranging from 0.15 to 0.45 mwe yr^{-1}. However, from 1910 to 1930 iodine summer concentrations did not change appreciably (Fig 1a) despite the wide range of annual thickness (Fig. S3 and S4). During this period, the summer iodine concentration was 0.030 ± 0.005 ng g^{-1} in samples where annual thickness was high (0.2 <ILT< 0.5 mwe) and 0.020 ± 0.007 ng g^{-1} in samples in which ILT was lower than 0.2 mwe. A similar small decrease in the iodine level with decreasing ILT was also observed in samples deposited from 1895 to 1910 (0.035 ± 0.010 ng g^{-1} for 0.1 <ILT< 0.2 mwe compared to 0.027 ± 0.007 ng g^{-1} for ILT< 0.1 mwe). Thus, although the Col du Dome record suggests a small post-depositional effect on iodine concentrations, we estimate that the summer iodine concentration in the ice increased by 0.01-0.02 ng g^{-1} from early 1890 to around 1905. This was followed by a decrease of 0.01-0.02 ng g^{-1} from the early to late 1930s.

Annual layer thickness in the CDD record increased in the late 20th century with only three summer layers of less than 0.5 mwe occurring after 1950 (Fig. S4**)** potentially contributing to the concurrent increases in CDD iodine concentrations. To accurately quantify changes in atmospheric iodine after 1950, summer iodine levels were separated into two sets based on their respective annual thickness (ILT<1.5 mwe and ILT>1.5 mwe). During the 1970-1980 decade when there were a number of years with ice layers in both ILT sets, iodine concentrations were consistently higher (0.042 ng g^{-1}) in summers with higher ILTs suggesting the post-depositional losses did indeed occur. Nevertheless, polynomial functions fit separately to the two ILT groups ($[I] = 3x10^{-203}\,[year]^{61.14}$ with $R^2 = 0.53$ blue triangles in Fig. 4; $[I] = 2x10^{-154}\,[year]^{46.29}$ with $R^2 = 0.5$ red circles in Fig. S4a), indicating a similar three to four-fold increasing trend between 1950 and 1995, (0.045 to 0.182 ng g^{-1} and from 0.030 to 0.088 ng g^{-1} for ILT>1.5 and ILT<1.5 mwe, respectively). From this analysis it is clear that even though part of the observed trend may be attributed changing snow deposition conditions, the CDD record suggests an increasing trend in summer atmospheric iodine of at least a factor of three from 1950 to 1995.

Seasonal changes in iodine concentration

Summer-to-winter differences in iodine could in theory be related to post-depositional smoothing of the atmospheric signal by diffusion in the firn. Indeed, because of its volatility, a large fraction of total iodine may be remobilized after deposition during firnification. If correct, a decrease in the summer-to-winter contrast would be expected when the distance between two adjacent summer snow layers is smaller, thereby allowing diffusion between high summer and low winter layers. This process would increase with depth because of the overall decrease of the annual (and winter-to-summer) snow deposition observed upstream of the CDD drill site. We calculated the half-year summer to winter ratio (S/W) as the mean half-year summer concentration observed during the two adjacent summers divided by the half-year winter concentration. As seen in Table S1, no systematic increase of the iodine winter concentration was observed when the

thickness of the winter layer was smaller; instead the main change in winter concentrations seemed to follow those in summer. For instance, despite a doubling of the winter layer thickness from the 1950-1960 to 1960-1970 decades, both winter and summer averaged levels remained unchanged (Table S1). Also, the further doubling of the winter layer thickness from the 1960-1970 to 1970-1980 decade was accompanied by an increase in winter levels parallel to an increase in summer.

Influences on atmospheric iodine concentrations unrelated to oceanic emissions

Among other iodine sources that may account for change in the iodine concentration of the CDD layers in the range of 0.01 ng g^{-1}, coal burning, volcanic activity, Saharan dust and kelp combustion for iodine production have to be considered.

Bettinelli et al. (2002) reported 1 to 4 ppm iodine in coal. Although there are numerous trace elements present in coal including halogens and various heavy metals that were measured in ice, their use is not straightforward to estimate the iodine content of coal combustion fallout in the ice. Indeed, heavy metals are far less volatile than halogens (boiling point of 184°C for iodine instead of 767° for cadmium or 1750°C for lead) and during combustion they mainly stay in fly ash particles whereas iodine is emitted as gaseous HI. Due to its very high solubility HI (a very strong acid) has a shorter atmospheric lifetime than fly ash containing metals. The use of trace metals therefore would strongly overestimate the iodine coal combustion fallout in the ice. Instead, given the short lifetime of iodine, to evaluate the role of coal burning we tentatively compare estimation of iodine coal burning emissions in France with the iodine deposition in alpine ice. Assuming a typical iodine content of coal of 2 ppm and given the mass of coal annually burnt in France between 1890 and 1950 (56,000 Gg, Fig. S5), we calculate that 110 tons (i.e., 0.11 Gg) of iodine are annually emitted from France by coal burning. If 10% of emissions are subsequently deposited over France, we estimate that around 10 tons of I are deposited per year on France. Assuming a typical precipitation of rate of 800 kg m^{-2}/yr^{-1} in France, we calculate a coal contribution of 0.02 ng g^{-1} in ice. Even though being uncertain, this calculation suggests that the impact of coal on iodine deposition has to be considered. As seen in Figure S5, the temporal fluctuations of iodine in ice did not follow those of coal burning emissions suggesting that natural oceanic emissions dominate coal burning. It has to be noted, however, that apart from the 1900-1910 decade possible slightly impacted by volcanic activity (see above), the ice iodine levels that were high in the early 30's when the coal consumption reached 80,000 Gg yr^{-1}, reached at absolute minimum in the early 40's when coal burning dropped to 40,000 Gg yr^{-1}. Note also the low iodine ice levels between 1915 and 1920 (Fig. S5).

Another source of atmospheric iodine was the practice of kelp burning used by the iodine industry along the west coast of Europe (in order of importance: Brittany in France, Norway, Scotland, Iceland, and Portugal). Iodine production reached a maximum in the early 1930s and then decreased to a minimum in 1939 (Cauer, 1939). For example, iodine production in France was 0.06 to 0.07 Gg yr^{-1} from 1909 to 1913. This production dropped by a factor of three during World War I (1914-1918) and increased up to 0.1 Gg yr^{-1} in 1934 before dropping again in the late 1930s. Changes of iodine production from kelp between 1890 and 1945 therefore tend to follow the coal burning changes in France. With 20-50% lost to the atmosphere during burning, Cauer (1939) estimated that 90 to

230 tonnes were released annually to the atmosphere in Western Europe prior to 1914. The annual emission of iodine due to kelp combustion may have reached 0.05 Gg in the early 30's in France, being significant compared to coal burning emissions at that time (0.16 Gg, Fig. S5). In conclusion, some of the observed small fluctuation seen in the iodine ice record, in particular the decreasing mean concentration between 1928-1931 (0.03 ng g^{-1}) and 1940-1943 (0.015 ng g^{-1}) possibly reflects the decrease of both coal burning and kelp combustion in France.

Finally, it is interesting to compare iodine emitted from coal burning and kelp combustion in France (reaching 0.21 Gg in 1930) with iodine emission from oceanic regions located offshore France. For instance, considering an oceanic area of 300 000 km^2 offshore France (Atlantic and Mediterranean Sea) the annual oceanic emissions in the pre-industrial time (Fig. S6) is close to 1.7 Gg compared to 0.12 Gg from coal burning (Fig. S5). Such a difference by one order of magnitude between oceanic and continental emissions would decrease, however, along the transport towards the Alps given the short atmospheric lifetime of iodine. This effect is clear when comparing surface mixing ratio due to oceanic emissions with a huge horizontal gradient for instance between the Mediterranean Sea and inland (Fig. S6).

Saharan dust

Saharan dust plumes sporadically reach the Alps and can be recognized in Alpine ice as alkaline calcium-rich layers (Wagenbach et al., 1996). Deposition of these plumes disturbed the level of numerous chemical species in the CDD ice because they either were present in dust at the emission stage or, being acidic, were taken up during transport by the alkaline material (Usher et al., 2003). Such plumes enhanced deposition of several cations (potassium, magnesium, and sodium) as well as acidic anions (sulfate, nitrate, chloride, fluoride, and carboxylates) (Preunkert, 2001), particularly in summer. We evaluated the acidity (or alkalinity) of samples by checking the ionic balance between major anions and cations with concentrations expressed in micro-equivalents per liter (μEq L^{-1}) as follows:

$$[H^+] = ([Cl^-] + [NO_3^-] + [SO_4^{2-}]) - ([Na^+] + [Mg^{2+}] + [Ca^{2+}] + [NH_4^+])$$

We emphasize that since calculations were made considering major ion data provided by the continuous measurements but ignoring the presence of mono- and di-carboxylates, the calculated acidity values are underestimated. As reported in Preunkert and Legrand (2013), the total contribution of carboxylates remained fairly stable through time accounting for ~5 μEq L^{-1} in summer CDD layers.

No significant relationship was found between the iodine content of CDD ice and Saharan dust arrivals. For instance, during the last decade for which summers were marked either by an absence or a large high Saharan dust input, no significant correlation was found between the concentration of iodine and the alkalinity (and/or the calcium content) of ice (R^2 = 0.04). The highest iodine level seen in 1990 (0.27 ng g^{-1}; Fig. 1a) corresponds to an acidic layer (5.6 μEq L^{-1}) containing a low calcium content (65 ng g^{-1}), whereas the iodine concentration in summer 1999 remained low (0.096 ng g^{-1}) despite a large Saharan dust input as indicated by its alkaline character (- 8.6 μEq L^{-1}) and a high calcium level (280 ng g^{-1}).

Volcanic eruptions

One specific event was seen in 1955 with an outstanding half-year summer iodine level of 0.13 ng g^{-1} compared to 0.04 ± 0.01 ng g^{-1} during the 1950-1960 decade (Fig. S3a) that was accompanied by an increase in bromine (1.7 ng g^{-1} instead of 1.0 ± 0.2 ng g^{-1} from 1950 to 1960). The date of the event and the relative amplitude of the two halogen perturbation (i.e., one order of magnitude larger for Br than I) suggest the Bezymianny eruption (Kamchatka, VEI of five, <citation: 10.1029/JC087iC02p01231>) in March 1956 as a possible cause. Indeed, recent satellite observations (Schönhardt et al., 2017) confirm previous estimates indicating that volcanoes emit on average ten times more bromine (5-15 Gg yr^{-1}) than iodine (0.5-2.0 Gg yr^{-1}) (Pyle and Mather, 2009). A sulfate perturbation in CDD ice also is expected, but its magnitude is difficult to quantify by checking half-year summer values (440 ng g^{-1} in 1955 compared to 370 ± 160 ng g^{-1} during the remaining part of the 1950-1960 decade). Our high-resolution record reveals the presence in summer 1955 of a thin ice layer (4 cmwe) characterized by a high acidity (17 EqL^{-1}) and containing 2180 ng g^{-1} of sulfate, 8.3 ng g^{-1} of Br, and 0.67 ng g^{-1} of I compared to 290 ng g^{-1}, 1.1 ng g^{-1}, and 0.07 ng g^{-1} during the remaining part of the summer, respectively. Again, showing a bromine perturbation ten times larger than the iodine, this thin layer revealed an input of sulfate corresponding to an SO_4/Br mass ratio of 315 (an SO_4/I ratio of 3150). The abundance of halogens relative to SO_2 in volcanic emissions depends on the tectonic environment, with halogen-rich emissions from volcanoes located in the subduction zones. On average for the subduction zones, an SO_2/HCl molar ratio ranging from 0.1 to 10 is reported by Halmer et al. (2002), with the lowest value for the Kamchatka zone. Using this latter SO_2/HCl molar ratio and a Br/Cl mass ratio ranging from 10^{-3} to 3.5 $x10^{-3}$ (Pyle and Marther, 2009), we calculate an SO_4/Br mass ratio of 80-270 at the emission stage. The 1955 perturbation in the CDD layers thus exhibits an SO_4/Br mass ratio that is in the upper range of values at the emission stage for the Kamchatka zone. Although the atmospheric lifetime of iodine within the troposphere (~2 days; Sherven et al., 2016) is shorter than bromine (18 days; Sherven et al. 2016) and sulfate (4-6 days), we cannot rule out that the 1955 CDD ice summer layers were impacted by the Benzyminaya eruption, with on average during summer an input of 50-150 ng g^{-1} of sulfate, 0.6 ng g^{-1} of bromine, and 0.06 ng g^{-1} of iodine.

The CDD ice may have recorded other volcanic eruptions including the large 1912-1913 Katmai event (Alaska, VEI of six). The CDD ice record does not reveal outstanding values of half-year summer iodine and sulfate levels over this period. The fact that the Bezymianny eruption may have resulted in a more marked sulfate perturbation than Katmai in the CDD ice is in line with the previous conclusion from Moore et al. (2012). They showed that, whereas in Greenland Katmai is well recorded and Bezymianny is seen as a small signal, Bezymianny is a prominent event in the ice from Svalbard and Severnaya Zemlya (Akadamii Nauk) (Opel et al., 2013). Furthermore, it is likely that the Katmai eruption was less rich in halogens relative to SO_2 than the Benzyminaya event. The SO_2/HCl ratio was not documented for the Alaska zone but to date, a value of the SO_2/HCl molar ratio of two (instead of 0.1 for Kamchatka) is proposed as an average for the whole subduction zone (Halmer et al., 2002).

Finally, we cannot rule out that the slightly higher iodine concentrations seen from 1904 to 1908 (0.05 and 0.044 ng g^{-1} in 1905 and 1906, respectively, Fig. S4) are partly related to volcanic events with high Volcanic Explosivity Indices (VEI,) including the eruption of Santa Maria (Guatemala, VEI of 6), Grimsvötn (Iceland, VEI of 4), and Ksudach (Kamchatka, VEI of 5).

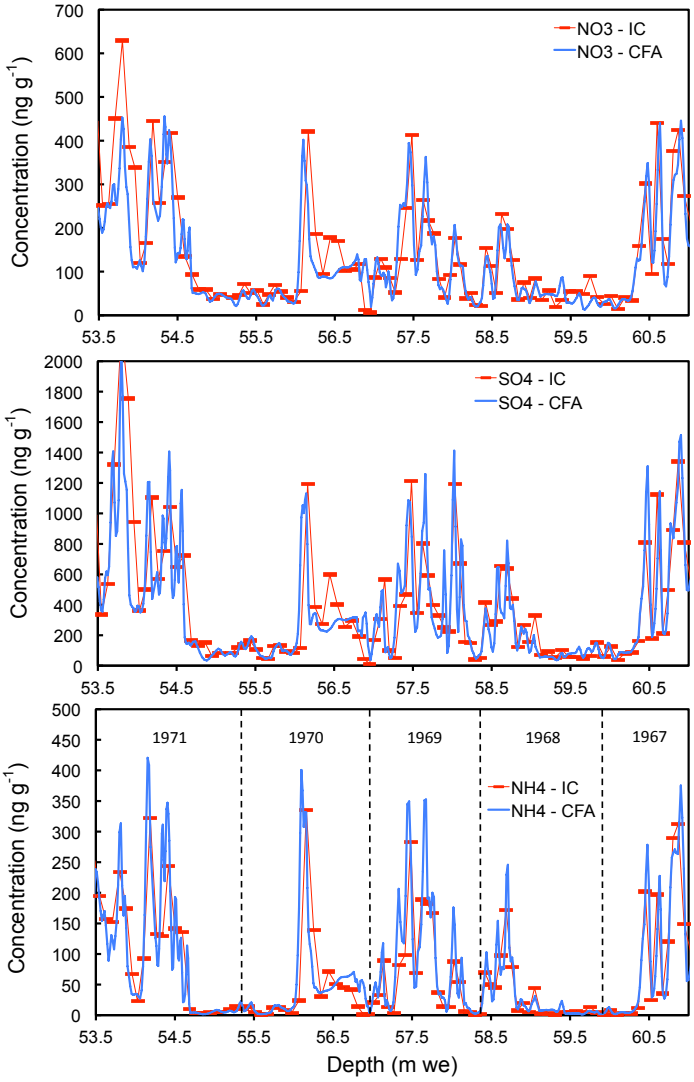

Fig. S1. Comparison of nitrate, sulfate, and ammonium concentrations measured in discrete samples using IC (red bars) and those measured with the CFA systems (blue lines) in ice from the CD10 core between 53.5 and 61.0 mwe depth (i.e., 1967-1971). S measurements made by ICP-MS multiplied by the sulfate to S mass ratio (3.0) were nearly identical to sulfate, indicating that other forms of S such as methane sulfonic acid (MSA) were negligible in CDD.

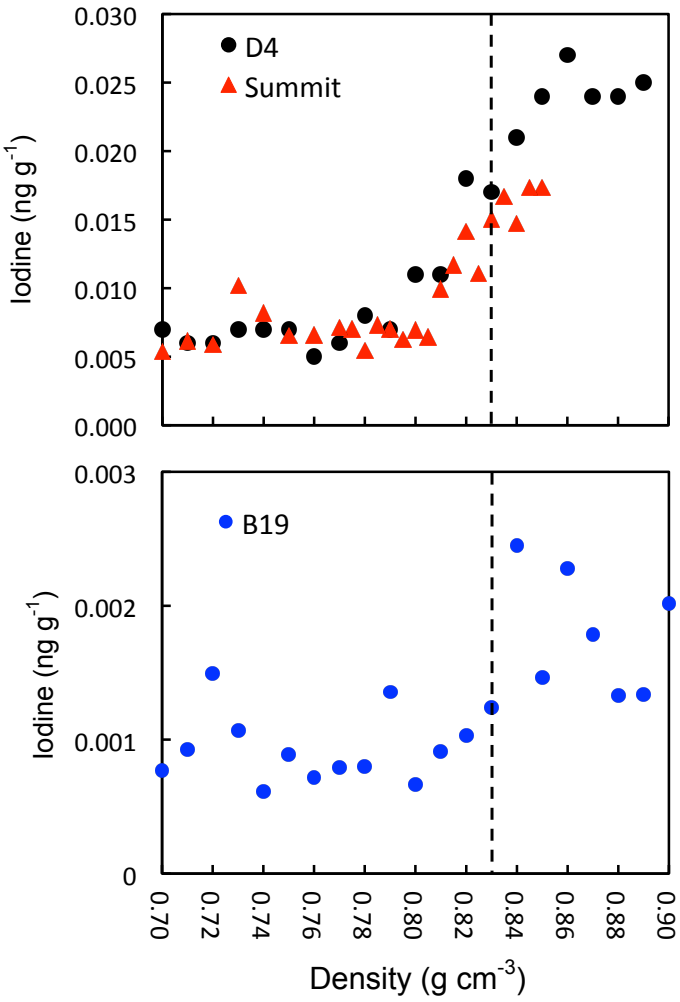

Fig. S2. Iodine concentrations as a function of the density of firn/ice cores extracted at three Greenland sites. The vertical dashed lines refer to the density at the firn-ice transition (i.e., 0.83 g cm^{-3}).

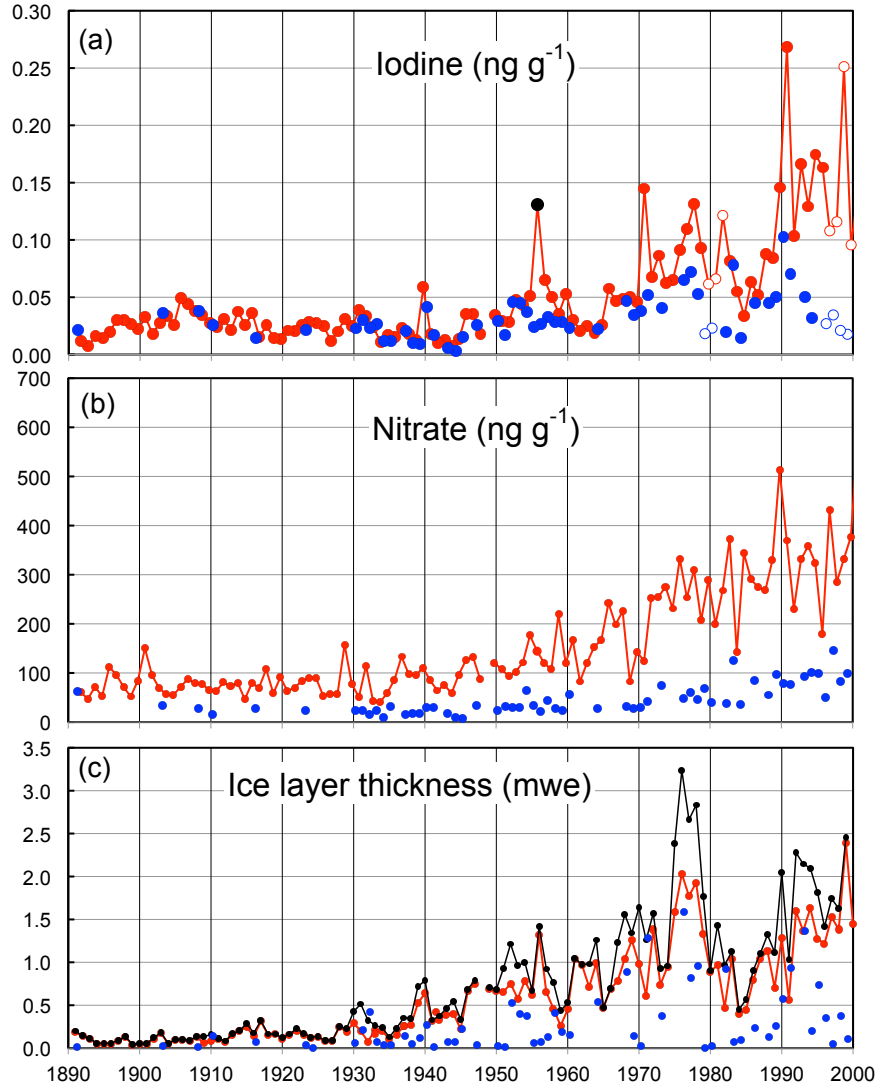

Fig. S3. Top and middle: Summer (red) and winter (blue) half-year means of iodine (a) and nitrate (b) along the CDD ice cores. Bottom: Ice layer thickness (c) along the CDD ice cores (summer [red], winter [blue], annual [black]). The winter value of iodine (0.156 ng g^{-1} in winter 1994/1995) was removed from the record. The black circle in (a) refers to the outstanding 1955 summer value. The open circle in (a) refer to firn layers.

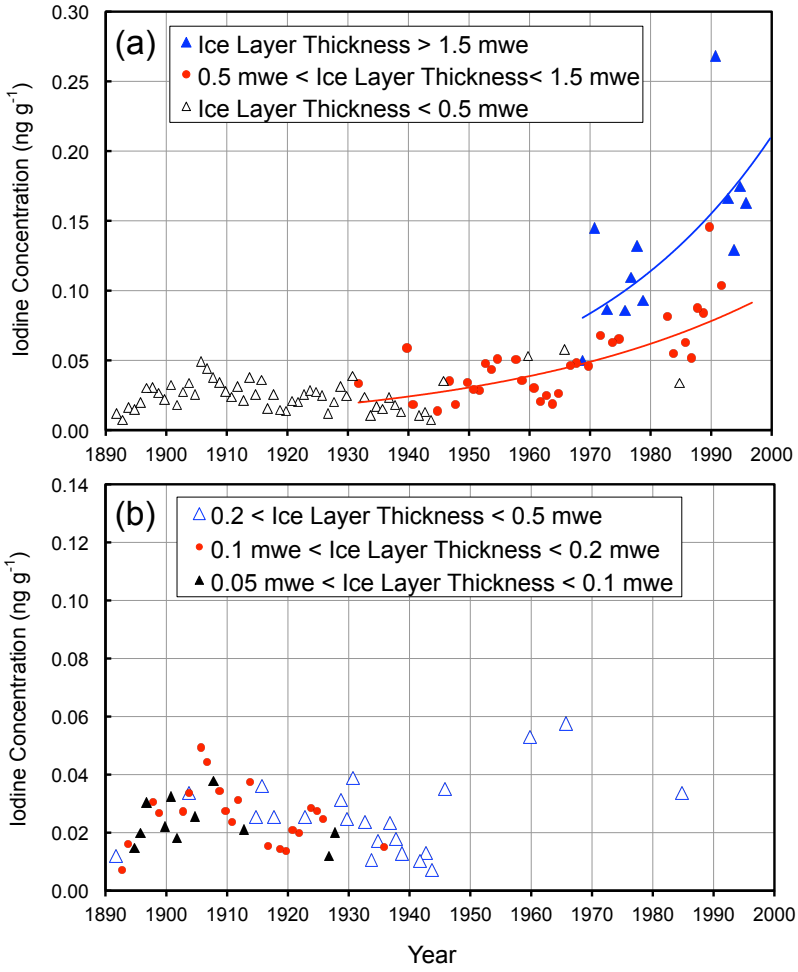

Fig. S4. Summer 1890 to 2000 iodine concentrations in CDD binned as a function of annual ILT (a): All ILT values, (b): ILT<0.5 mwe. The red and blue lines show polynomial fits. Summer 1995 and 1948 were not considered as well as all measurements in firn (see SI Appendix text).

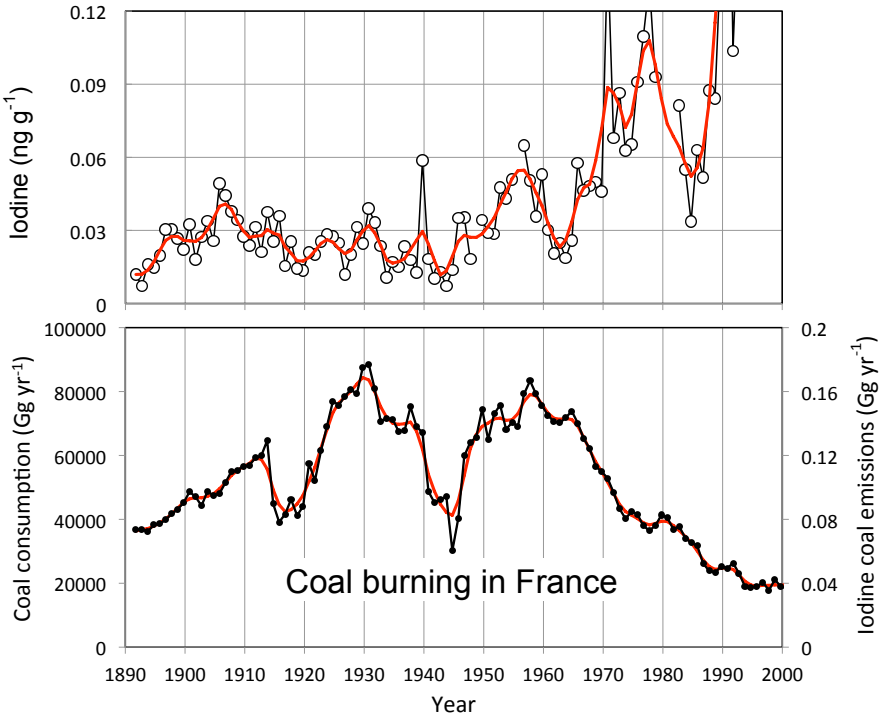

Fig. S5. Summer iodine trend in CDD ice together with historical coal consumption in France from 1890 to 2000. For iodine (top) the thin line and open points (black) are individual summer half-year means, the solid thick line (red) the first component of a single spectra analysis (SSA) with a three-year time window. Annual mass of coal burning in France between 1890 and 1975 are from Mitchell (1978) and from British Petroleum from 1975 to 2000 (http://tools.bp.com/energy-charting-tool).

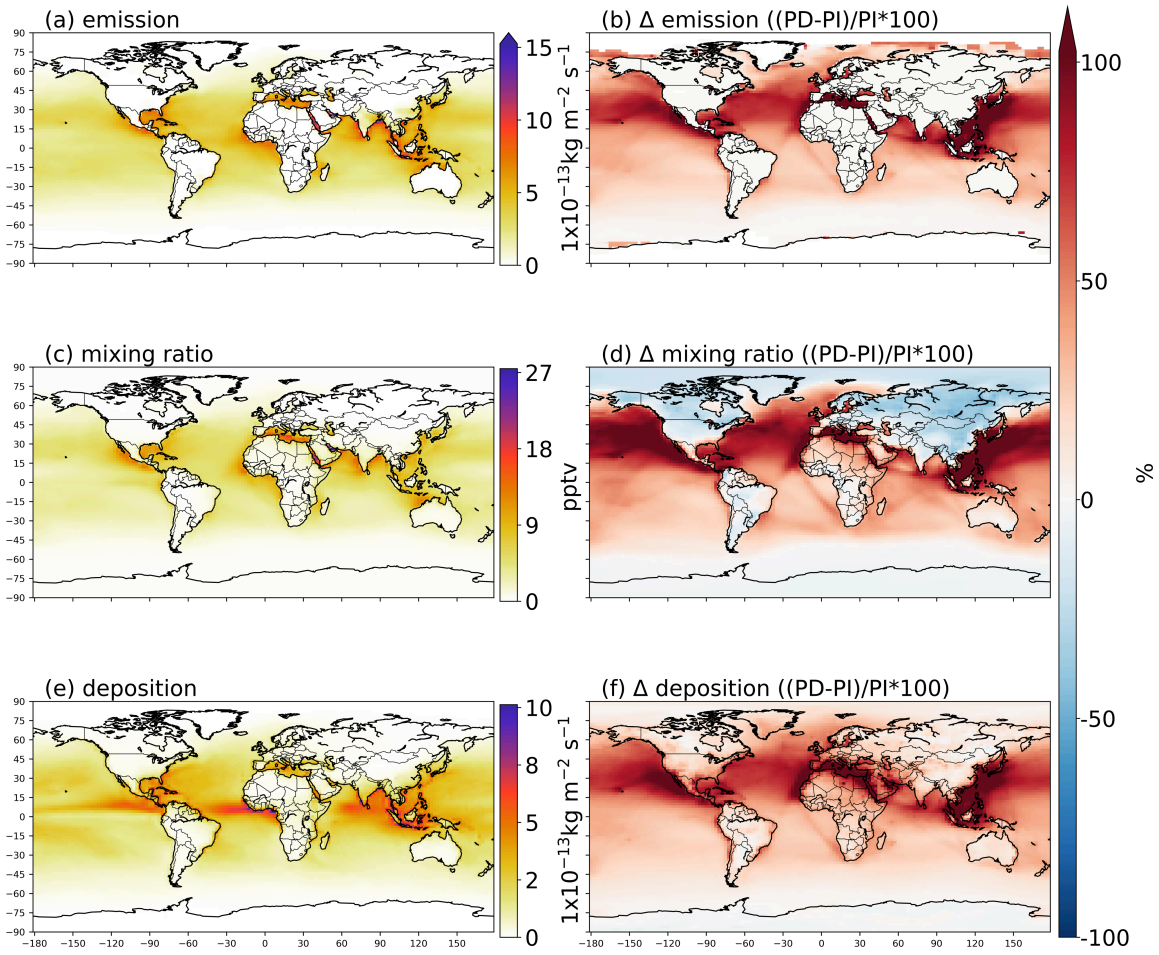

Fig. S6. a,b: Simulated oceanic I_y annual mean emission for present-day (PD) and percentage change from the preindustrial (PI) to PD. c,d: surface annual mean I_y mixing ratios for the PD and percentage change from the PI to PD. e,f: I_y annual mean deposition for the PD and percentage from the PI to PD.

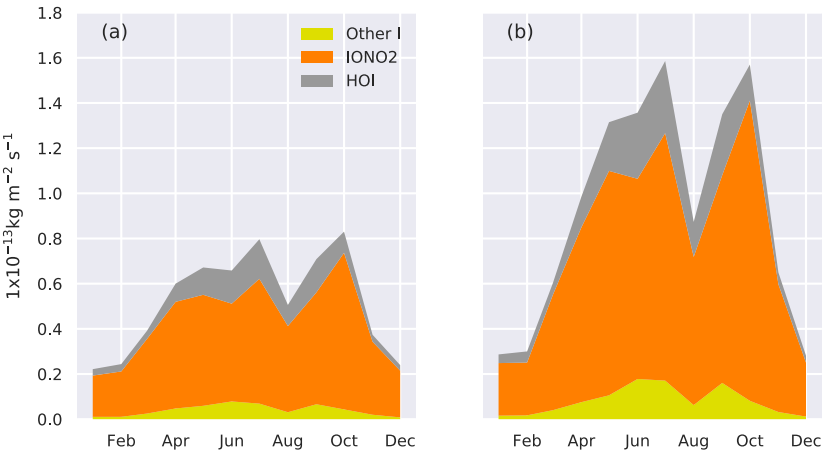

Fig. S7. Seasonality of speciation of iodine deposition at CDD for (a) the present day (PD) with preindustrial (PI) iodine emissions and (b) the PD with PD iodine emissions.

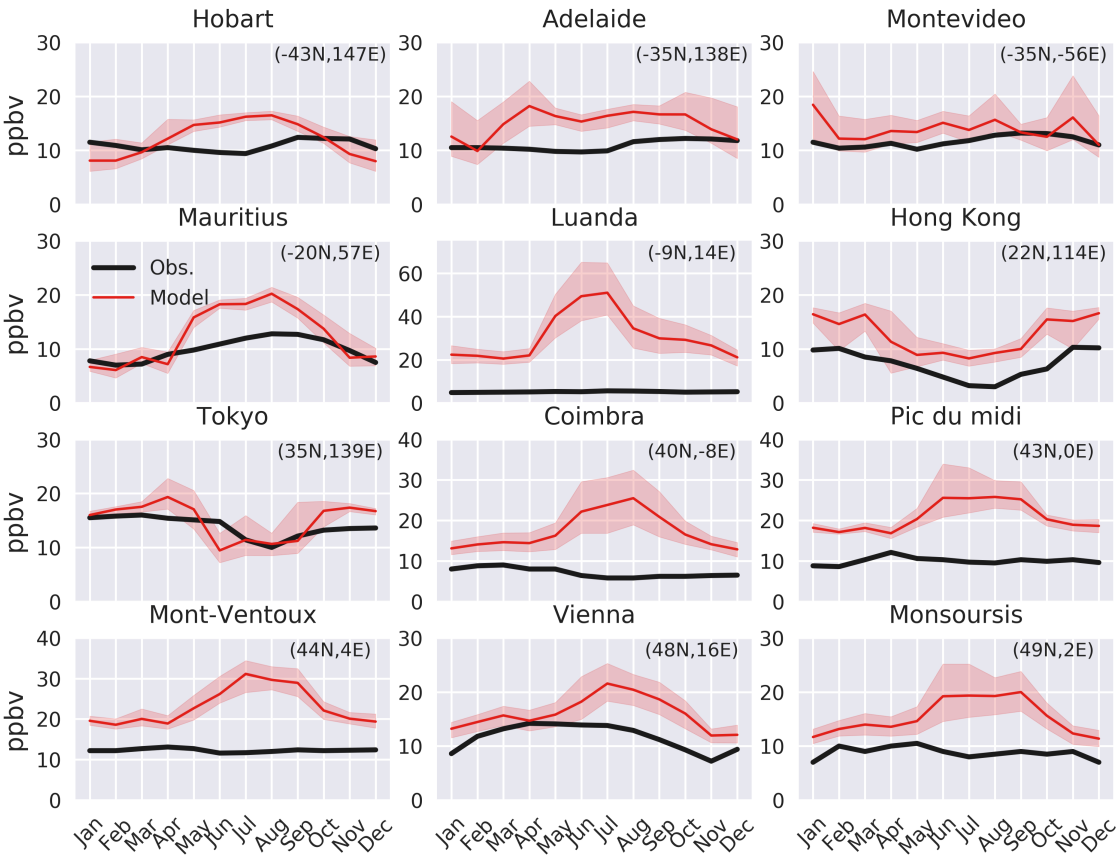

Fig. S8. Comparison between seasonal observed and modelled preindustrial ozone. Observations are shown in black and model in red. The shaded areas for the model simulation show the first and third quartiles in the hourly values. The model results are in broad agreement with those from other models simulating PI ozone by using the ACCMIP emissions (see Figure 2 in Stevenson et al., 2013). The ozone data are reproduced from previously reported observations (Mickley et al., 2001): Mont Ventoux, Hong Kong, Tokyo, Adelaide, Coimbra, Hobart, Luanda, Mauritius, Vienna, and Montevideo (Marenco et al., 1994); Pic du Midi (Pavelin et al., 1999); Montsouris (Volz and Kley, 1988).

Table S1. Change through time of the summer (S) to winter (W) iodine contrast along with winter ice layer thickness (ILT_{winter}).

Decade	ILT_{winter} (mwe)	I_{winter} (ng g^{-1})	I_{summer} (ng g^{-1})	S/W
1930-1940	0.13	0.018	0.023	1.5
1940-1950[a]	0.12	0.018	0.019	1.6
1950-1960[a]	0.22	0.031	0.039	1.3
1960-1970	0.43	0.032	0.039	1.3
1970-1980	0.84	0.052	0.095	2.0
1980-1990	0.28	0.038	0.066	1.9
1990-1995[b]	0.98	0.073	0.168	2.6

[a] Summer 1955 and 1948 were not considered

[b] The outlier winter 1994-1995 was removed from calculations

References

1. Hutterli, M. A., McConnell, J. R., Bales, R. C., and Stewart, R. W. (2003). Sensitivity of hydrogen peroxide (H2O2) and formaldehyde (HCHO) preservation in snow to changing environmental conditions: Implications for ice core records. J. Geophys. Res., 108(D1), 4023, doi:10.1029/2002JD002528.
2. Legrand M., Léopold, A., and Dominé, F. (1996). Acidic gases (HCl, HF, HNO3, HCOOH, and CH3COOH): A review of ice core data and some preliminary discussions on their air-snow relationships. In NATO ASI Ser., "Processes of chemical exchange between the atmosphere and polar snow," Vol. I43, E. Wolff and R.C. Bales eds., Springer-Verlag, 19-44.
3. Frieß, U., Deutschmann, T., Gilfedder, B. S., Weller, R., and Platt, U. (2010). Iodine monoxide in the Antarctic snowpack. Atmos. Chem. Phys., 10, 2439-2456, doi:10.5194/acp-10-2439-2010, 2010.
4. Spolaor, A., Vallelonga, P., Gabrieli, J., Martma, T., Björkman, M. P., Isaksson, E., Cozzi, G., Turetta, C., Kjær, H. A., Curran, M. A. J., Moy, A. D., Schönhardt, A., Blechschmidt, A.-M., Burrows, J. P., Plane, J. M. C., and Barbante, C. (2014). Seasonality of halogen deposition in polar snow and ice. Atmos. Chem. Phys., 14, 9613-9622, doi:10.5194/acp-14-9613-2014.
5. Maselli, O. J., Chellman, N. J., Grieman, M., Layman, L., McConnell, J. R., Pasteris, D., Rhodes, R. H., Saltzman, E., and Sigl, M. (2017). Sea ice and pollution-modulated changes in Greenland ice core methanesulfonate and bromine. Clim. Past, 13, 39-59, doi:10.5194/cp-13-39-2017.
6. Preunkert, S., Wagenbach, D., and Legrand, M. (2003). A seasonally resolved Alpine ice core Record of Nitrate: Comparison with Anthropogenic Inventories and estimation of Pre-Industrial Emissions of NO from Europe. J. Geophys. Res., 108, D21, 4681, doi : 10.1029/2003JD003475.
7. Legrand, M., Preunkert, S., Wagenbach, D., Cachier, H., and Puxbaum, H. (2003). A historical record of formate and acetate from a high elevation Alpine glacier: Implications for their natural versus anthropogenic budgets at the European scale. J. Geophys. Res., 108, D24, 4788, doi : 10.1029/2003JD003594.
8. Legrand, M., Preunkert, S., May, B., Guilhermet, J., Hoffman, H., and Wagenbach, D. (2013). Major 20th century changes of the content and chemical speciation of organic carbon archived in Alpine ice cores: Implications for the long-term change of organic aerosol over Europe. J. Geophys. Res. Atmos., 118, doi:10.1002/jgrd.50202.
9. Leuchner, M., Ghasemifard, H., Lüpke, M., Ries, L., Schunk, C., and Menzel, A. (2016). Seasonal and Diurnal Variation of Formaldehyde and its Meteorological Drivers at the GAW Site Zugspitze. Aerosol and Air Quality Research, doi: 10.4209/aaqr.2015.05.0334.
10. Gilbert, A., Gagliardini, O., Vincent, C., and Wagnon, P. (2014). A 3-D thermal regime model suitable for cold accumulation zones of polythermal mountain glaciers. J. Geophys. Res. Earth Surf., 119, doi:10.1002/2014JF003199.
11. Bettinelli, M., Spezia, S., Minoia, C., and Ronchi, A. (2002). Determination of chlorine, fluorine, bromine, and iodine in coals with ICP-MS and IC. At. Spectrosc., 23, 105-110.
12. Cauer, H. (1939). Schwankungen der Jodmenge der Luft in Mitteleuropa, deren Ursachen und deren Bedeutung für den Jodgehalt unserer Nahrung. Angew. Chem., 52, 625-628.
13. Wagenbach, D., Preunkert, S., Schaefer, J., Jung, W., and Tomadin, L. (1996). Northward transport of Saharan dust recorded in a deep Alpine ice core. in: The impact of African dust across the Mediterranean, edited by: Guerzoni, S. and Chester, R., Kluwer Academic Publishers, The Netherlands, 291-300.

14. Usher, C. R., Michel, A. E., and Grassian, V. H. (2003). Reactions on mineral dust. Chem. Rev., 103, 4883-4939, https://doi.org/10.1021/cr020657y, 2003.
15. Preunkert, S. (2001). L'histoire de la pollution atmosphérique Européenne reconstituée à partir des carottes de glace Alpine. Ph. D. thesis, 240 pp., Univ. Joseph Fourier de Grenoble, France.
16. Preunkert, S., and Legrand, M. (2013). Towards a quasi-complete reconstruction of past atmospheric aerosol load and composition (organic and inorganic) over Europe since 1920 inferred from Alpine ice cores. Clim. Past, 9, 1403-1416, doi:10.5194/cp-9-1403-2013.
17. Schönhardt, A., Richter, A., Theys, N., and John P. Burrows, P. P. (2017). Space-based observation of volcanic iodine monoxide. Atmos. Chem. Phys., 17, 4857-4870, doi:10.5194/acp-17-4857-2017.
18. Pyle, D. and Mather, T. (2009). Halogens in igneous processes and their fluxes to the atmosphere and oceans from volcanic activity: a review. Chem. Geol., 263, 110-121, doi:10.1016/j.chemgeo.2008.11.013.
19. Halmer, M. M., Schmincke, H.-U., and Graf, H.-F. (2002). The annual volcanic gas input into the atmosphere, in particular into the stratosphere: a global data set for the last 100 years. J. of Volcanology and Geotherma Res., 1115, 511-528.
20. Sherwen, T., Schmidt, J. A., Evans, M. J., Carpenter, L. J., Großmann, K., Eastham, S. D., Jacob, D. J., Dix, B., Koenig, T. K., Sinreich, R., Ortega, I., Volkamer, R., Saiz-Lopez, A., Prados- Roman, C., Mahajan, A. S., and Ordóñez, C. (2016). Global impacts of tropospheric halogens (Cl, Br, I) on oxidants and composition in GEOS-Chem. Atmos. Chem. Phys., 16, 12239-12271, doi:10.5194/acp-16-12239-2016.
21. Moore, J. C., Beaudon, E., Kang, S., Divine, D., Isaksson, E., Pohjola, V. A., and van de Wal, R. S. W. (2012). Statistical extraction of volcanic sulphate from nonpolar ice cores. J. Geophys. Res., 117, D03306, doi:10.1029/2011JD016592.
22. Opel, T., Fritzsche, D., and Meyer, H. (2013). Eurasian Arctic climate over the past millennium as recorded in the Akademii Nauk ice core (Severnaya Zemlya). Clim. Past, 9, 2379-2389, doi:10.5194/cp- 9-2379-2013.
23. Mickley, L. J., Jacob, D. J., and Rind, D. (2001). Uncertainty in preindustrial abundance of tropospheric ozone: Implications for radiative forcing calculations, J. Geophys. Res.-Atmos., 106, 3389-3399, doi:10.1029/2000JD900594.
24. Marenco, A., Gouget, H., Nédélec, P., Pagés, J.-P., and Karcher, F. (1994). Evidence of a long-term increase in tropospheric ozone from Pic du Midi data series: Consequences: Positive radiative forcing, J. Geophys. Res.-Atmos., 99, 16617-16632, doi:10.1029/94JD00021.
25. Pavelin, E. G., Johnson, C. E., Rughooputh, S., and Toumi, R. (1999). Evaluation of pre-industrial surface ozone measurements made using Schönbein's method, Atmos. Environ., 33, 919-929, doi:10.1016/S1352-2310(98)00257-X.
26. Volz, A. and Kley, D. (1988). Evaluation of the Montsouris series of ozone measurements made in the nineteenth century, Nature, 332, 240-242, doi:10.1038/332240a0.
27. Stevenson, D. S., Young, P. J., Naik, V., Lamarque, J.-F., Shindell, D. T., Voulgarakis, A., Skeie, R. B., Dalsoren, S. B., Myhre, G., Berntsen, T. K., Folberth, G. A., Rumbold, S. T., Collins, W. J., MacKenzie, I. A., Doherty, R. M., Zeng, G., van Noije, T. P. C., Strunk, A., Bergmann, D., Cameron-Smith, P., Plummer, D. A., Strode, S. A., Horowitz, L., Lee, Y. H., Szopa, S., Sudo, K., Nagashima, T., Josse, B., Cionni, I., Righi, M., Eyring, V., Conley, A., Bowman, K. W., Wild, O., and Archibald, A. (2013). Tropospheric ozone changes, radiative forcing and attribution to emissions in the Atmospheric Chemistry and Climate Model Intercomparison Project (ACCMIP), Atmos. Chem. Phys., 13, 3063-3085, https://doi.org/10.5194/acp-13-3063-2013.